An *In Situ* HVEM Study of Dislocation Generation at Al/SiC Interfaces in Metal Matrix Composites

MARY VOGELSANG, R. J. ARSENAULT, and R. M. FISHER

Annealed aluminum/silicon carbide (Al/SiC) composites exhibit a relatively high density of dislocations, which are frequently decorated with fine precipitates, in the Al matrix. This high dislocation density is the major reason for the unexpected strength of these composite materials. The large difference (10:1) between the coefficients of thermal expansion (CTE) of Al and SiC results in sufficient stress to generate dislocations at the Al/SiC interface during cooling. In this *in situ* investigation, we observed this dislocation generation process during cooling from annealing temperatures using a High Voltage Electron Microscope (HVEM) equipped with a double tilt heating stage. Two types of bulk annealed composites were examined: one with SiC of discontinuous whisker morphology and one of platelet morphology. In addition, control samples with zero volume percent were examined. Both types of composites showed the generation of dislocations at the Al/SiC interface resulting in densities of at least 10^{13} m^{-2}. One sample viewed end-on to the whiskers showed only a rearrangement of dislocations, whereas, the same material when sectioned so that the lengths of whiskers were in the plane of the foil, showed the generation of dislocations at the ends of the whiskers on cooling. The control samples did not show the generation of dislocations on cooling except at a few large precipitate particles. The results support the hypothesis that the high dislocation density observed in annealed composite materials is a result of differential thermal contraction of Al and SiC. The SiC particles act as dislocation sources during cooling from annealing temperatures resulting in high dislocation densities which strengthen the material.

I. INTRODUCTION

THE incorporation of 20 vol pct discontinuous SiC whiskers into a 6061 Al matrix increases the yield strength of annealed powder compacted 6061 Al alloy by more than a factor of two. This increase in strength cannot be explained directly by continuum mechanics theories. Continuum mechanics formulations developed by Piggott[1] and applied to the case of discontinuous Al/SiC composites by Arsenault[2] predict an ultimate strength of only 186 MPa for 20 vol pct SiC composite, whereas the measured value of ultimate strength for this material is 448 MPa. Arsenault and Fisher[3] proposed that the increased strength could be accounted for by a high dislocation density in the Al matrix which is observed in bulk composite material annealed for as long as 12 hours at 810 K.

The dislocation generation mechanism proposed by Arsenault and Fisher to account for this high dislocation density is based on the large difference (10:1) in coefficients of thermal expansion (CTE) of Al and SiC.[4] When the composite is cooled from elevated temperatures of annealing or processing, misfit strains occur due to differential thermal contraction at the Al/SiC interface which are sufficient to generate dislocations.

Chawla and Metzger, in an elegant investigation of Cu/W composites using etch-pitting techniques, observed a high dislocation density at the Cu/W interface which decreased with increasing distance from the interface.[5] They observed that if the volume fraction of W was 15 pct, the minimum dislocation density in the matrix was 7×10^{11} m^{-2} increasing to 4×10^{12} m^{-2} at the interface of W and Cu, and concluded that the dislocations were caused by the differences (4:1) in CTE of Cu and W. Recalling that the CTE difference between Al and Si is 10:1, *i.e.*, more than twice as great as the Cu/W system, one would expect thermal stresses in Al/SiC to be sufficient to generate dislocations in this composite.

Other causes may also contribute to the high dislocation density observed in annealed Al/SiC material. Dislocations are introduced into this material during the plastic deformation processes of manufacturing, such as extrusion. During annealing, the dislocations introduced during processing may not be annihilated; they could be trapped by the SiC, resulting in a high dislocation density after annealing.

It is important to determine the origins of the high dislocation density in the composite since the strength of the composite depends on the high density. If the differential thermal contraction is the cause of the dislocations, as Arsenault and Fisher[3] suggest, then dislocations should be observed being generated in a composite thin foil sample on cooling from annealing temperatures in an *in situ*, HVEM experiment.

In situ dynamic HVEM experiments have certain advantages over other experimental techniques. The major advantage is that direct observation of a dynamic process altering a microstructure is possible while the deforming force, in this case a thermal stress, is operating. Operating at higher voltages allows penetration of thicker samples so that surface effects are minimized and bulk behavior is more closely approximated. Also, a high voltage microscope can better accommodate special stages required for *in situ* work because of the large pole piece region.

Numerous *in situ* HVEM heating stage investigations of Al have been performed. Hale *et al.*[6] and Caillard and Martin[7] investigated dislocation motion during creep at

MARY VOGELSANG and R. J. ARSENAULT, Director, are with the Metallurgical Materials Laboratory, University of Maryland, College Park, MD 20742. R. M. FISHER is with Center for Advanced Materials, Lawrence Berkeley Laboratory, University of California, Berkeley, CA 94720.

Manuscript submitted April 8, 1985.

elevated temperatures using HVEM. Kivilahti *et al.*[8] observed an Al-2 pct Mg alloy *in situ* during recovery processes at elevated temperatures recording dislocation interactions on videotape. Shimotomori and Hasiguti[9] observed *in situ* prismatic punching of dislocation loops at second phase precipitates in an Al-1.3 pct Li alloy. Electron irradiation of Al at elevated temperatures has been extensively studied using HVEM.[10,11]

There have been several non-dynamic, non-*in situ* TEM investigations of dislocations about particles in a metal matrix. Weatherly[12] observed multiple slip mode dislocation tangles around silica in Cu, and concluded they were caused by differential thermal contraction of the two materials on quenching. Ashby *et al.*[13] observed dislocations about pressurized silica-Cu, noting a critical size dependence for dislocation generation. Williams and Garmong[14] reported a high incidence of dislocations at the Ni/W interface in this directionally solidified eutectic composite.

Calculations of the dislocation density in Al/SiC due to thermal stresses predict high dislocation densities. The misfit strain which develops at the circumference of a 1 μm diameter SiC particle due to differential thermal contraction during cooling is approximately 1 pct. The plastic strain at one-half the interparticle spacing, obtained from Lee *et al.*,[15] ranges from 1 to 2 pct. The dislocation density can be simply calculated from the following equation:

$$\varepsilon_p = \rho L b . \qquad [1]$$

where ε_p is the plastic strain (1 pct), ρ is the dislocation density (m^{-2}) generated, L is the average distance moved by the generated dislocations, which was taken to be 1/2 the inter-whisker spacing, *i.e.*, 2 μm, and b is the Burgers vector of Al. The ρ obtained is 1.8×10^{13} m^{-2}.

Consideration of another type of dislocation described by Ashby[16] predicts additional dislocations in the matrix. These dislocations are called "geometrically necessary" dislocations by Ashby, and occur in order to allow compatible deformation of a system with geometrical constraints such as hard particles which do not deform as the surrounding ductile matrix. These geometrically necessary dislocations are required if the deformation takes place without the formation of voids about the hard particles. Slip dislocations are a function of the material properties of the system, and are not dependent on the microstructural constraints. According to Ashby, the density of geometrically necessary dislocations, ρ^G, is given by:

$$\rho^G = \frac{4\gamma}{\lambda^G b} \qquad [2]$$

where λ^G is the "geometrical slip distance" analogous to the slip distance in pure crystals. For platelet particles, λ^G is equal to the length of the plate and γ is the shear strain. For a 1 pct shear strain and $\lambda^G = 4$ μm, ρ^G equals approximately 3×10^{13} m^{-2}. Taking these dislocations into account results in a further addition to the predicted dislocation density in the Al matrix.

The purpose of this investigation was to determine if dislocation generation occurs at the Al/SiC interface on cooling a composite from annealing temperatures, and to determine if the observed densities of dislocations generated during cooling are in agreement with densities predicted by theoretical calculations.

II. MATERIAL

Three types of material were examined. The first was a SiC whisker composite purchased from ARCO-Silag. It is a powder metallurgy product: 6061 Al alloy powder is compressed with SiC whiskers to form a billet; then the billet is extruded to align the whiskers and form a 12.5 mm diameter rod. Three different volume fractions of SiC were considered: 0 pct, 5 pct, and 20 pct. The zero vol pct material served as a control.

The second type of composite was purchased from DWA, and contains SiC of platelet morphology. The platelets are 5 to 7 μm long and have an aspect ratio of two to three. This composite is also a powder metallurgy product supplied in the form of a plate, and the third type of material was wrought 1100 grade Al in the form of a 12.5 mm diameter rod, and it was in the as-received condition. This material also served as a control.

III. SAMPLE PREPARATION AND EXAMINATION PROCEDURE

An ion milling technique was required for the production of TEM samples due to the SiC in the Al matrix.

These two types of composite and the 0 vol pct control were machined into rods (12 mm in diameter, 4 cm long), annealed for 12 hours at a solutionizing temperature of 810 K, and furnace cooled. After annealing, slices of 0.76 mm thickness were cut by electric discharge machining (EDM) at 80 to 100 V. Deformation damage from EDM is estimated to extend 0.20 mm beneath the surface.[17,18] The slices were fixed to a brass block with double-sided tape and surrounded by brass shims, then mechanically thinned on a rotating water flooded wheel covered with 400 then 600 grit paper to remove the EDM damage and reduce the thickness to approximately 0.127 mm. Final thinning was carried out using argon ion plasma bombardment, operating at 6 kV, and ion current of 50 micro amperes and a sample inclination of 15 deg to the ion beam. For these operating parameters the projected range, or average distance the argon ion travels into the foil, is only 20 nm.[19,20] Dupuoy[21] conducted an *in situ* ion thinning experiment on Fe and Al-Ag specimens using a 3 MV microscope. Dislocation arrangements and microstructures in Al-Ag and Fe were not altered by ion thinning even though some point defects are introduced into the near surface region of the sample by ion bombardment. Therefore, it can be concluded that ion-milling does not introduce or remove dislocations in the TEM foils.

The 1100 grade Al control samples were prepared from the as-received wrought rod in the same manner as the composite samples, except electro-polishing was employed instead of ion-thinning.

The thinned samples were then observed in the HVEM operating at 800 kV with a beam current of 2.3 μA. A double tilt, side-entry, furnace type heating stage was used to heat the specimen. While being observed in the microscope, the samples were heated to 800 K and held for 15 minutes, then cooled to ambient temperature. Subgrains exhibiting dislocations in contrast were chosen for observation. During heating and cooling, thermal drift of the stage and thermal expansion and contraction of the sample caused the chosen subgrain to move. In order to maintain the

same subgrain in the field of view at the same crystallographic orientation, it was necessary to slightly translate and tilt the specimen almost continuously. Since changing to SAD conditions during cycling to monitor orientation would have resulted in loss of the chosen area from the field of view, the orientation was maintained constant by monitoring the contrast of microstructures such as a subgrain boundary or SiC/Al interface in the bright-field mode. One thermal cycle required about one hour, and most of the samples were observed throughout several thermal cycles. The thickest regions of the sample penetrated by the beam were chosen for observation, and at operating voltage of 800 KV the beam will penetrate 0.8 μm thick Al.[22] The dislocation density, ρ, was determined by a line intercept method adapted from Hale.[23] A grid of lines is placed over the TEM micrograph, then the intersections of dislocation lines with the grid lines are counted. The dislocation density, ρ, is given by

$$\rho = \frac{2N}{LT}$$

where N is the number of dislocation intersections with the grid lines, L is the length of the grid lines divided by the magnification, t is the thickness of the sample (0.8 μm), and the length of the lines on the grids was 0.58 m. Each reported dislocation density is an average value obtained from 3 to 10 micrographs.

IV. RESULTS

The discussion of the experimental results will be divided into three parts: 0 vol pct, 5 vol pct, and 20 vol pct of SiC. In all cases, typical results will be described. A total of 800 micrographs were taken.

A. *Controls, 0 Vol Pct SiC, 6061 Al, and 1100 Al*

The 0 vol pct 6061 Al control sample had a large subgrain size (approximately 5 μm) and a low dislocation density (8×10^{12} m^{-2}) (Figure 1(a)). A few of the larger second phase precipitate particles (Mg_2Si) were surrounded by dislocation tangles bowing out from the precipitate interface (Figure 1(b)). On heating, the dislocations began to move in the sample, migrating away from the particles. Other dislocations were also generated in other areas of the subgrain and moved through the matrix, occasionally being pinned by precipitate particles. Eventually, at elevated temperatures (670 K), all of the dislocations disappeared. Slip traces left behind when the dislocations moved also disappeared at temperatures close to 700 K, possibly due to surface diffusion. The sample was held at 800 K for about 15 minutes.

The image tended to be out of focus at high temperatures due to thermal drift of the stage (Figures 1(b) and 1(c)). On cooling, dislocations reappeared at the large particle interface at about 500 K, sometimes moving faster than could be seen. The dislocations formed tangles in the vicinity of the precipitate; however, most of the matrix did not accumulate any dislocations (Figure 1(d)). There were a few dislocations generated at subgrain or grain boundaries.

The 1100 Al sample had a dislocation density initially of 4×10^{12} m^{-2}, and a large subgrain size, 5 μm (Figures 2(a) and 2(b)). Thicker regions containing few precipitates were chosen for observation. On heating, most of the dislocations had disappeared upon reaching 673 K. At this temperature, the heating stage mechanism failed; therefore, the sample never reached 800 K, but heating was sufficient to remove the dislocations from the area under observation. The dislocations in this area did not return on cooling, except a few which were connected to precipitate particles (Figures 3(a) and 3(b)).

B. *5 Vol Pct—Transverse and Longitudinal Whisker SiC*

The 5 vol pct whisker sample, sectioned transverse to the whiskers so that the hexagonal whiskers are viewed end-on in the microscope, had a small subgrain size, 2.0 μm, and a high dislocation density, 4×10^{13} m^{-2}, in the subgrains (Figure 4(a)). In this case, on heating the dislocations did not disappear but straightened from an initially bowed configuration and became more regularly spaced: a polygonized configuration. These dislocations did not disappear at high temperatures (Figures 4(b) and 4(c)). On cooling, the dislocations again bowed away from the Al/SiC interface but the density of dislocations did not increase; if anything, the number slightly decreased (Figures 4(d) and 4(e)). Several of the subgrains appeared to change shape during the thermal cycle; however, their boundaries did not move past the surrounding SiC whiskers.

The longitudinal 5 vol pct sample, sectioned parallel to the SiC whisker axis so that the whiskers could be viewed lengthwise, did show the characteristic disappearance of dislocations at high temperatures, and then the return of dislocations on cooling, especially at the ends of the whiskers (Figures 5(a) through (f)). The parallel lines in the whiskers have been previously identified as microtwins.[24]

C. *20 Vol Pct Whisker and Platelet*

The microstructure of the 20 vol pct whisker sample before heating is characterized by a small subgrain size of the order of 2 to 3 μm and also by a dislocation density of about 10^{13} m^{-2} (Figure 6(a)). The sample was heated while focusing on a single subgrain surrounded by several SiC whiskers. The dislocations began to move and rearrange, some moving very quickly, and eventually disappearing. Upon reaching 470 K most of the dislocations had disappeared. The sample was heated further to 800 K (Figure 6(b)), held for a few minutes, and then cooled. On cooling, dislocations reappeared and emanated from the whisker interface forming a tangle of dislocations in the small subgrain. Although some dislocations began appearing on cooling at about 473 K, a great number of them formed at temperatures less than 373 K. The dislocation density after cooling was comparable to the dislocation density before the thermal cycle (Figures 6(c), 6(d), and 6(e)). When black spots began obscuring the picture, another area free of the black spots was moved into the field of view.

The 20 vol pct platelet sample (Figure 7(a)) exhibited behavior similar to the whisker sample, in that most of the dislocations disappeared upon reaching 650 K (Figure 7(b)), and then on cooling, dislocations reappeared (Figures 7(c) and 7(d)). However, certain aspects of the microstructural alterations on cooling were peculiar to the platelet sample. In the first cycle, the dislocations disappeared and then reappeared on cooling. An unusual subgrain was observed

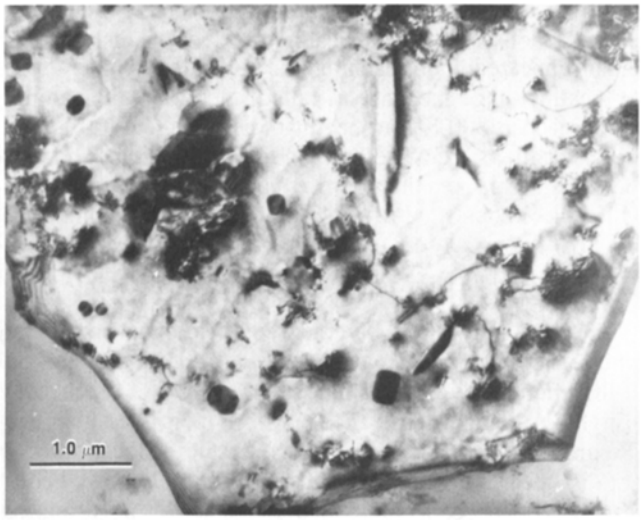

(a)

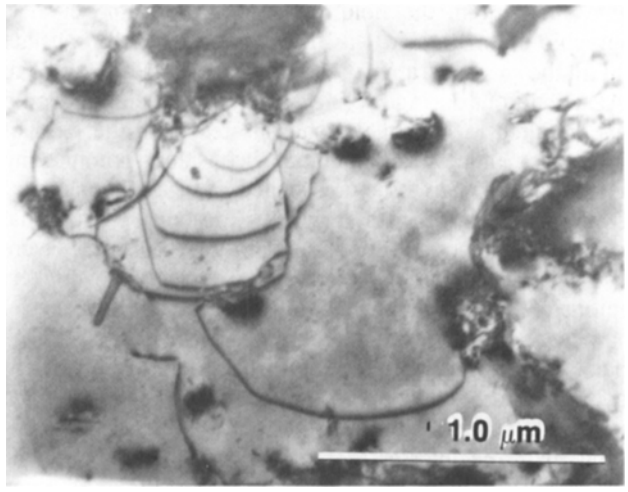

(b)

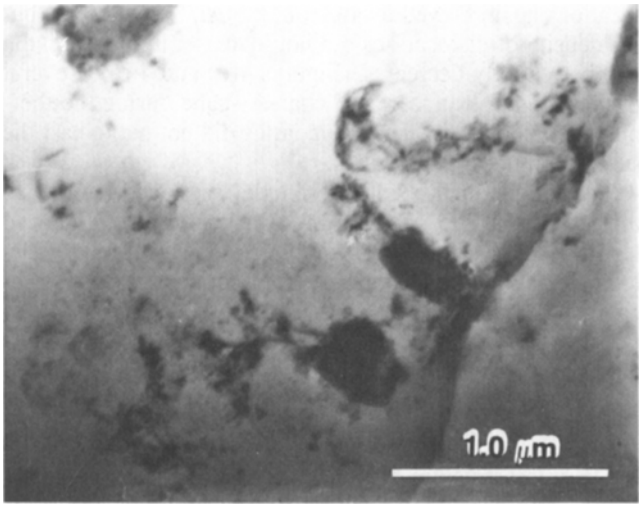

(c)

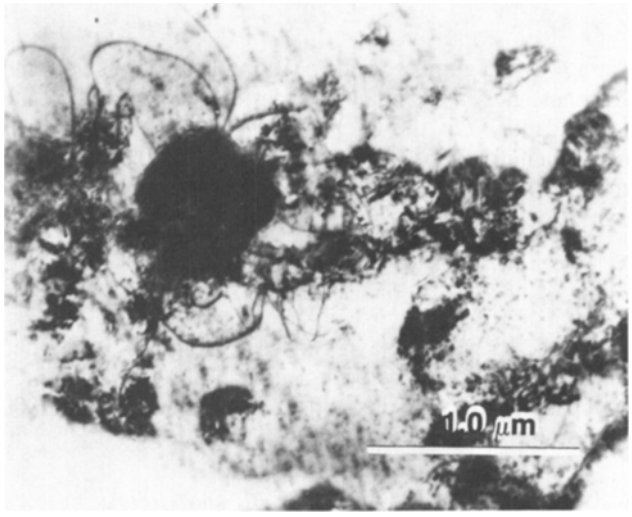

(d)

Fig. 1 — (*a*) Micrograph of a control sample illustrating the low dislocation density and the large grain size of annealed powder compacted 6061 Al with no SiC. The few dislocations present in this control sample are associated with the second phase precipitates of the 6061-Al alloy. Compare the dislocation densities and subgrain sizes with those of composites shown in Figs. 4(a), 6(a), and 7(a). (*b*) A large second phase precipitate (top center) surrounded by dislocations at the beginning of the thermal cycle (340 K). (*c*) As temperature increased to annealing temperatures in the microscope (780 K), the dislocations gradually disappeared until only a few remained (same area as Fig. 1(b)). (*d*) During *in situ* cooling of the control sample, dislocations reformed in the area of the precipitates, shown here. However, most of the matrix remained free of dislocations (same area as Figs. 1(a) and 1(b)).

which was filled with slip traces. This area was chosen as the area of focus in the next cycle. The parallel lines disappeared on heating; then on subsequent cooling, packets of slip traces appeared emanating from the SiC platelet. The slip traces formed in three directions at angles of about 82 deg and 45 deg to each other and were associated with dislocations which had appeared. The dislocations causing the slip traces moved too rapidly to be seen. After the third thermal cycle, many subgrains were filled with slip traces originating at the SiC platelet interface.

D. *Dislocation Densities*

The dislocation densities of all samples before and after *in situ* annealing are shown in Table I. The densities are higher in the composite samples than in the control samples both before and after *in situ* thermal cycling, *i.e.*, annealing. However, the dislocation densities reported are lower limit densities. There was difficulty in taking selected area diffraction patterns of a given subgrain and then tilting to a specific reflection, *i.e.*, ⌊420⌋ and assuring that the same orientation was maintained throughout. Therefore, the reported densities could be ½ to ⅓ of the actual density.[25]

The distribution of the dislocations within the samples was not uniform; there was a higher density, as to be expected, near the SiC. Also greater dislocation generation was observed at larger SiC platelets and whiskers than at the smaller ones, and more dislocations were generated at the ends of the SiC whiskers where plastic strain during cooling is greatest, than at the middle of the whisker length. The dislocation generation in the platelet sample was much greater than the dislocation generation in the

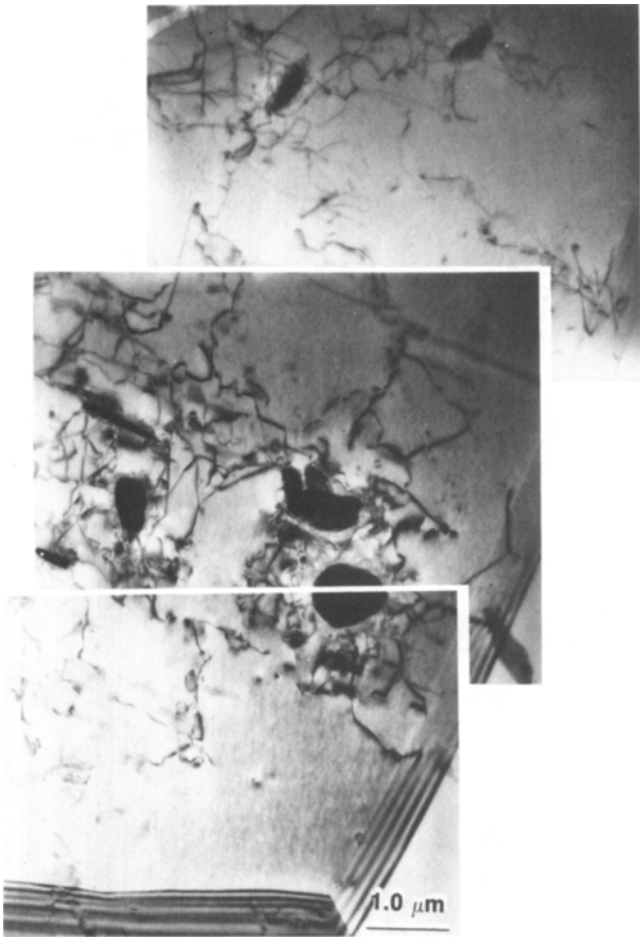

(*a*)

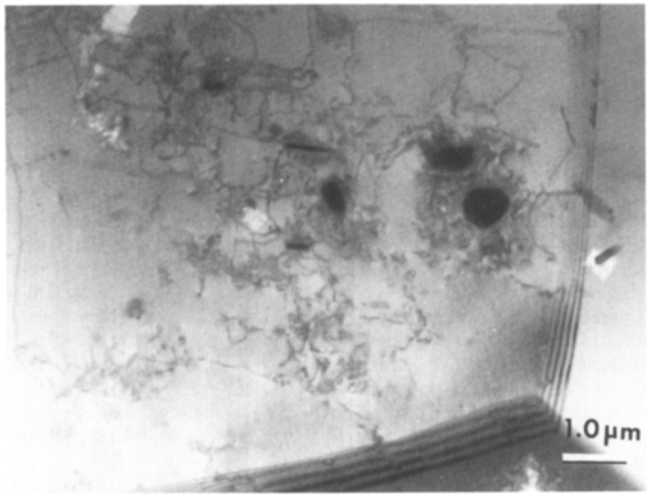

(*b*)

Fig. 2—(*a*) Wrought 1100 Al control sample, as-received condition. Before *in situ* thermal cycling, this control sample with no SiC had a high dislocation density. Like the 6061 Al control, this sample has a large grain size, and the dislocations present are often associated with precipitates. The white structure is a corrosion tunnel from electropolishing. (*b*) Low magnification view of 1100 control sample including area of Fig. 2(a).

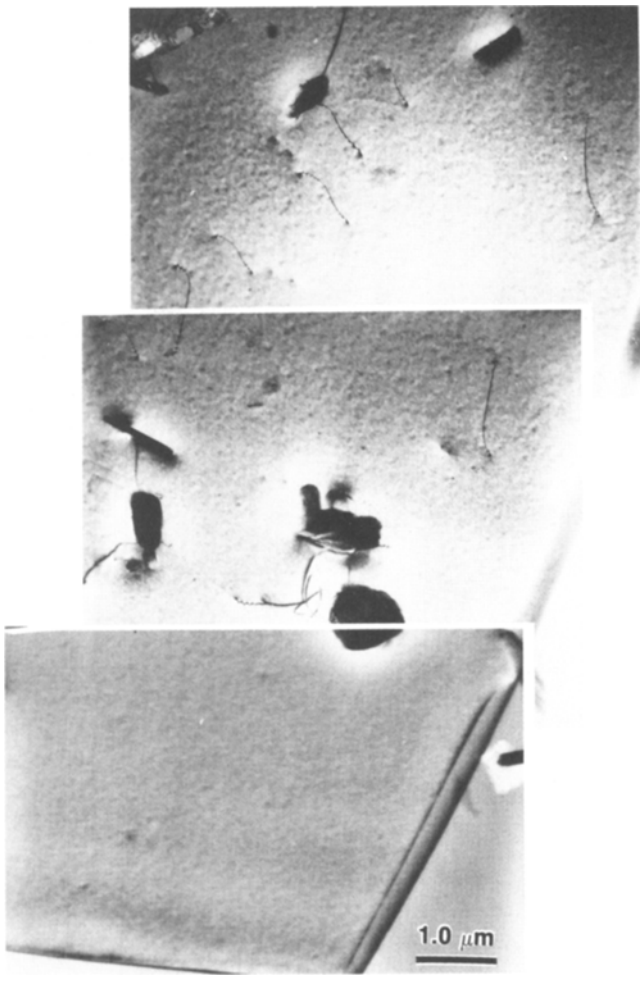

(*a*)

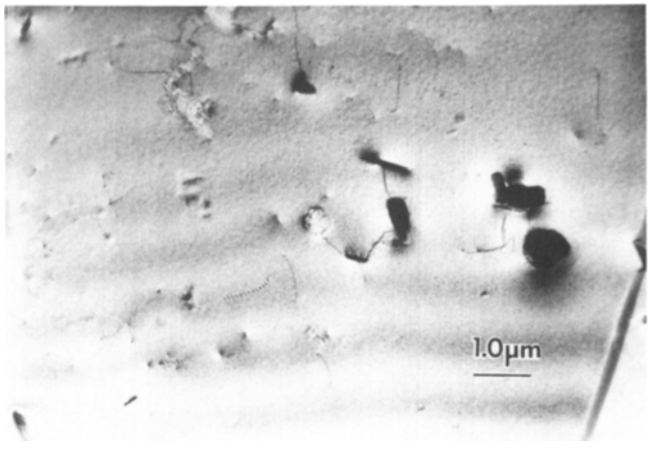

(*b*)

Fig. 3—(*a*) The same areas in Fig. 2(a) after *in situ* thermal cycling. In the absence of SiC, few dislocations reappear in a thermally cycled sample; the few dislocations present are associated with second phase precipitate particles.(*b*) Low magnification view of area in Fig. 3(a) after thermal cycling.

(*a*)

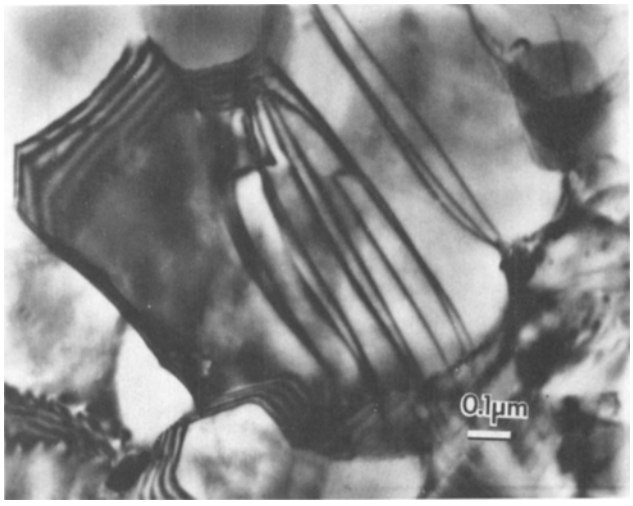

(*b*)

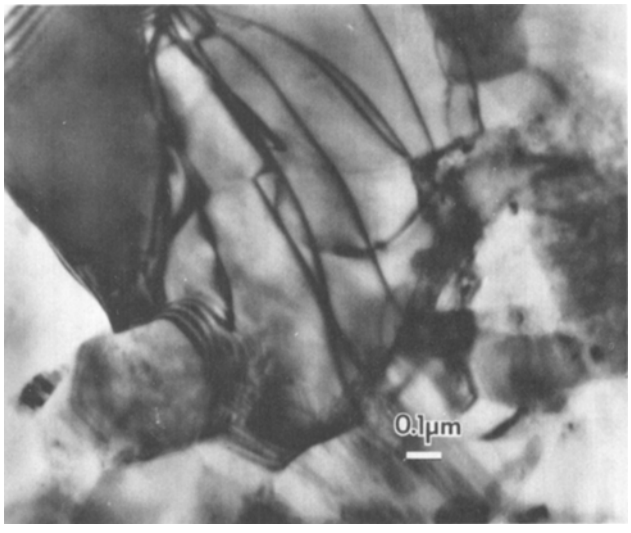

(*c*)

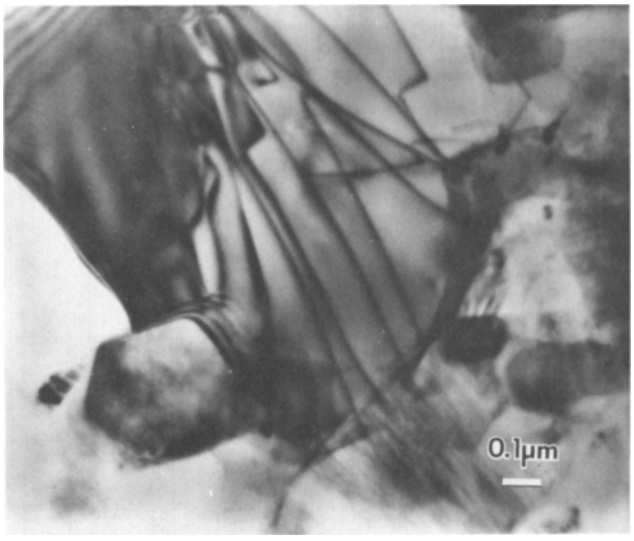

(*d*)

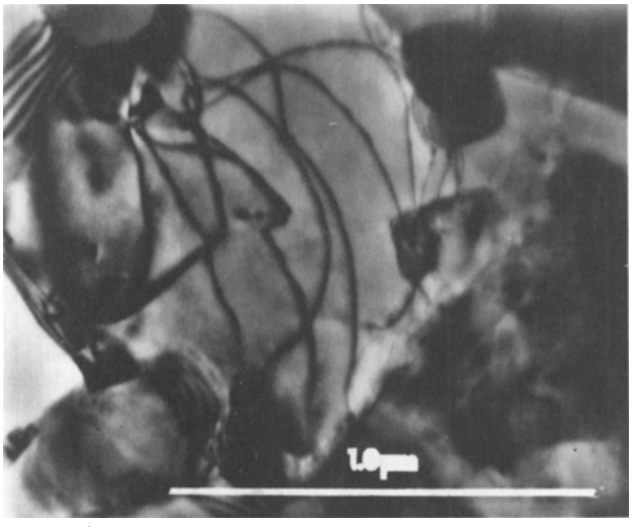

(*e*)

Fig. 4—(*a*) A foil cut transverse to the whisker axis (5 vol pct SiC). At the beginning of the thermal cycle, 370 K, the dislocations tended to bow away from the two hexagonal SiC whiskers. (*b*) The dislocations straighten on further heating to 570 K (same area as Fig. 4(a)). (*c*) Further rearrangement of the dislocations occurred on heating to the annealing temperature of 800 K in the microscope. The dislocations straightened and moved to more equally spaced positions (same area as Figs. 4(a) and 4(b)). (*d*) During cooling to 570 K the dislocations again began to bow away from the SiC whiskers (same area as Figs. 4(a-c)). (*e*) On cooling to 360 K, the curvature of the dislocations became pronounced, indicating the operation of a thermal stress; however, the generation of new dislocations did not occur (same area as Figs. 4(a-d)).

whisker samples, for SiC platelets are about 5 times larger than SiC whiskers.

As a consequence, of all the dislocation generation, there is a possibility of void formation at the SiC-Al interface. Voids were not observed in any of the samples.

V. DISCUSSION

The presence of SiC particles of either whisker or platelet morphology in an Al metal matrix composite resulted in the generation of dislocations at the Al/SiC interface when the

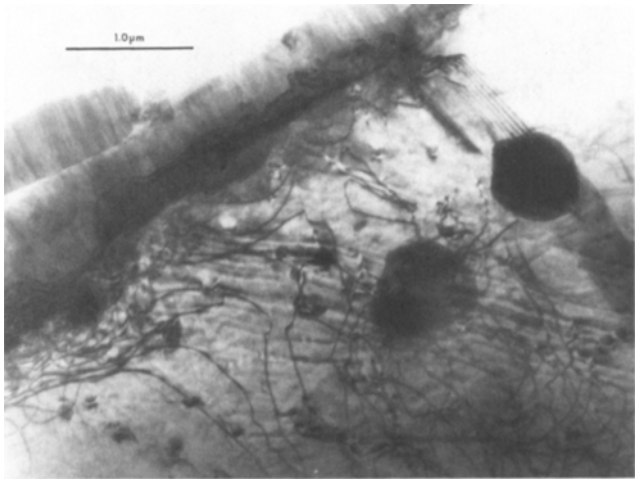

(*a*)

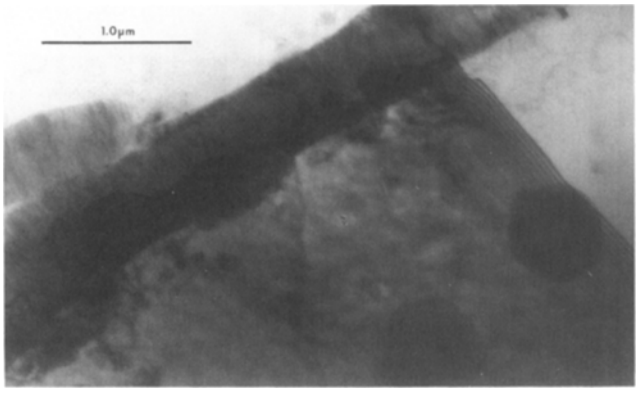

(*c*)

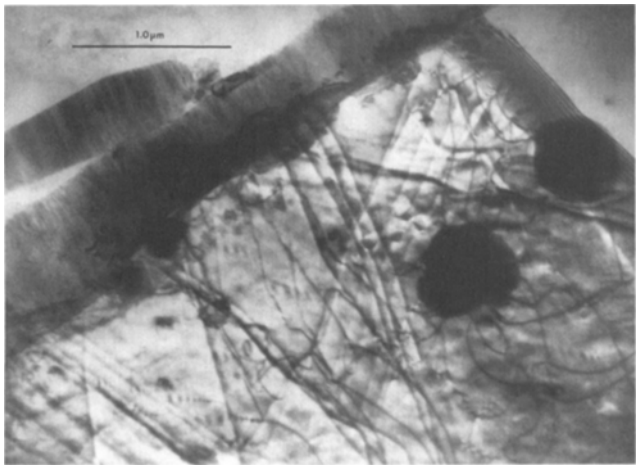

(*e*)

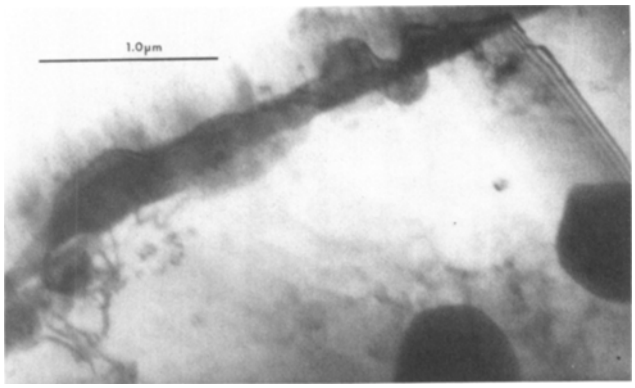

(*b*)

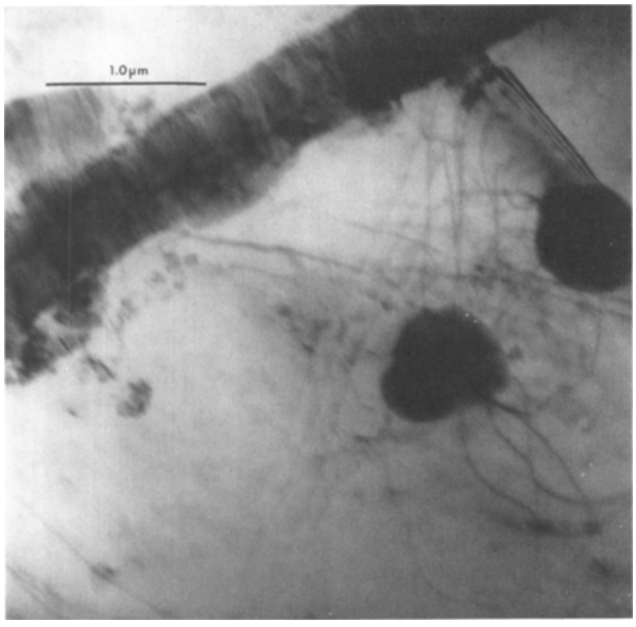

(*d*)

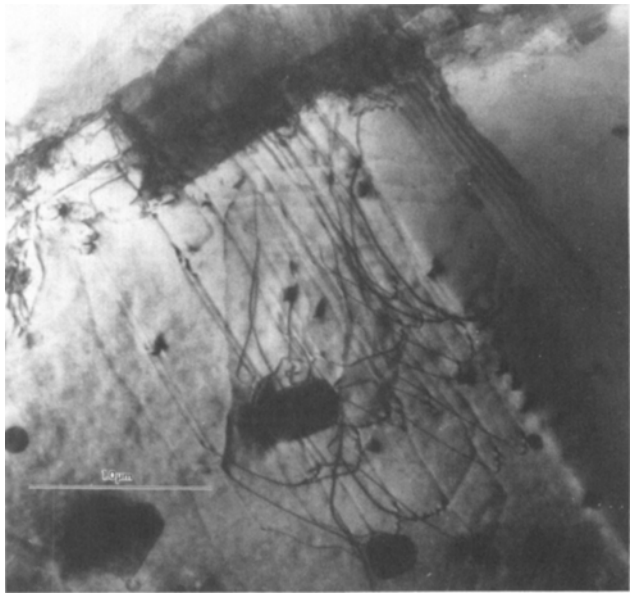

(*f*)

Fig. 5 - -(*a*) This sample was prepared from the same 5 vol pct whisker material shown in Figs. 4(a-e), only sectioned parallel to the SiC whisker axis. Dislocations are associated with the SiC and second phase precipitates at the beginning of the thermal cycle at 340 K. Also visible are parallel slip traces from the previous thermal cycle. (*b*) The same region at annealing temperature, 810 K, after most dislocations have disappeared. (*c*) The same area after one dislocation has reappeared on cooling to 580 K. (*d*) On further cooling the sample to 480 K, more dislocations have formed, some leaving slip traces as they moved away from the Al/SiC interface. (*e*) On cooling to 430 K, dislocation activity greatly increased as evidenced by the higher density of dislocations and slip traces. (*f*) Another location in the sample at 340 K which also shows dislocation generation clearly associated with the SiC. This area was not irradiated by the electron beam during the thermal cycle.

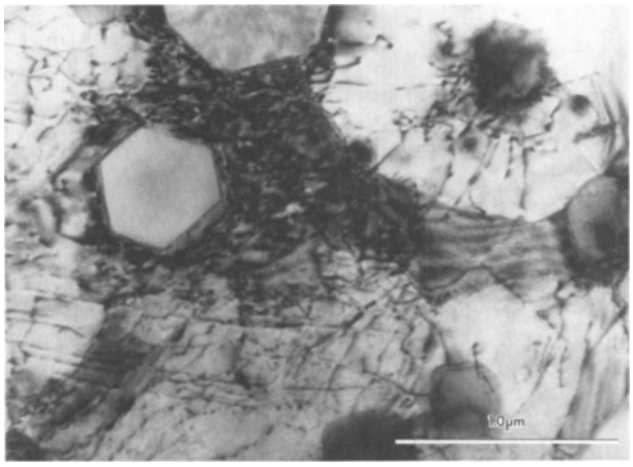

(*a*)

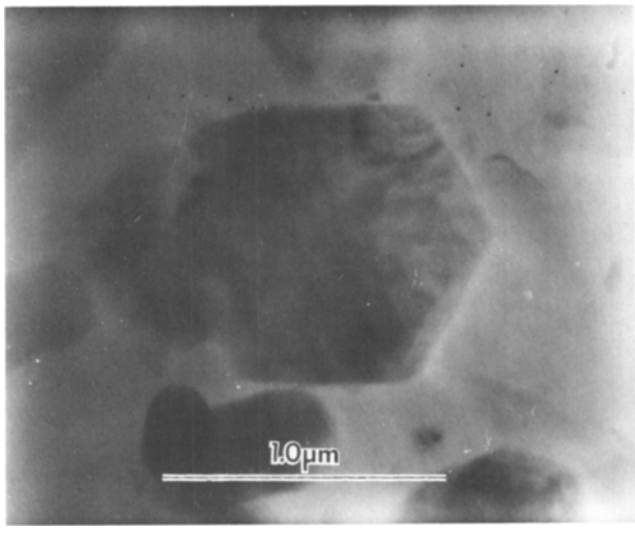

(*b*)

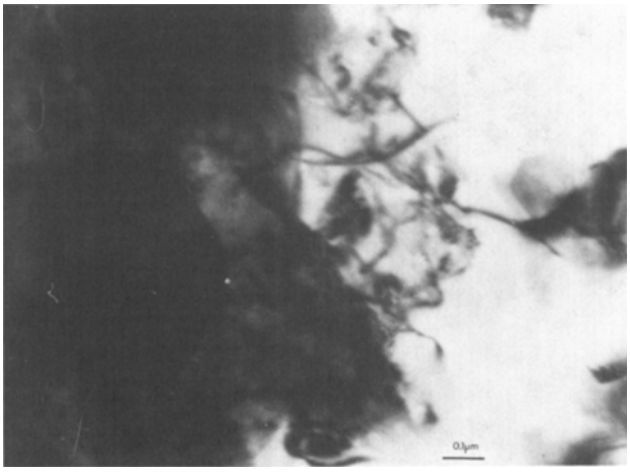

(*c*)

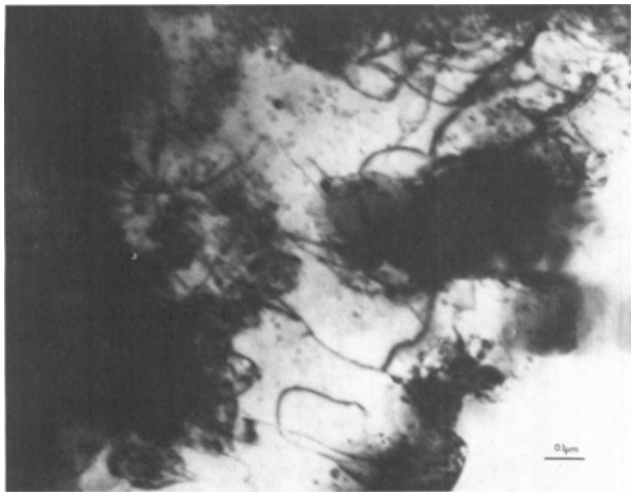

(*d*)

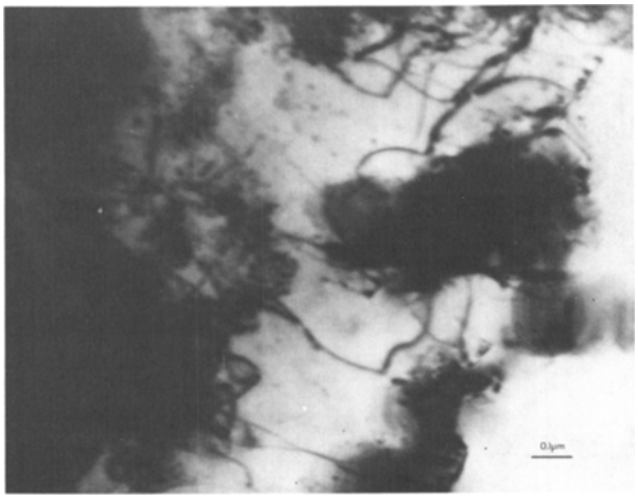

(*e*)

Fig. 6—(*a*) The initial high dislocation density and small subgrain size of the 20 vol pct whisker composites is shown here. (*b*) The dislocations disappeared from the sample during *in situ* heating to 800 K. Thermal drift of the stage prevented sharp focusing of the image. (*c*) On cooling to 375 K, dislocations had reappeared in the sample, emanating from the Al/SiC interface and moving into the matrix until a dislocation tangle formed. (*d*) The clear area at 375 K (Fig. 6(c)) as temperature decreased to 340 K. Black spots also began to form on the sample at this temperature. (*e*) At lower center, the appearance of a hook-shaped dislocation is observed. The black spots have become more prominent, 330 K.

composite was cooled from the annealing temperature. In general, the high density of dislocations originally present in the composite samples disappeared at 500 to 650 K, then reappeared on cooling at densities close to the high densities originally observed in the annealed specimens. In contrast, dislocations were not generated to the same extent in either of the control samples during cooling.

The small subgrain size and high dislocation densities previously observed by Arsenault and Fisher[7] can be associated with the presence of the SiC in the composite, specifically the CTE differential. The difference in CTE resulted in stresses large enough to cause plastic deformation, *i.e.*, the generation of dislocations. These dislocations can be defined as slip dislocations. Dislocation generation is also required to accommodate the heterogeneous plastic flow in the vicinity of the deforming matrix since voids are not observed. We can conclude, therefore, that both of

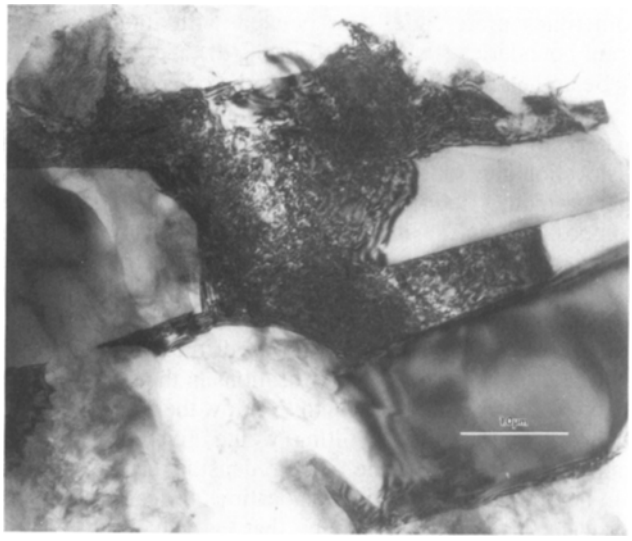

(a)

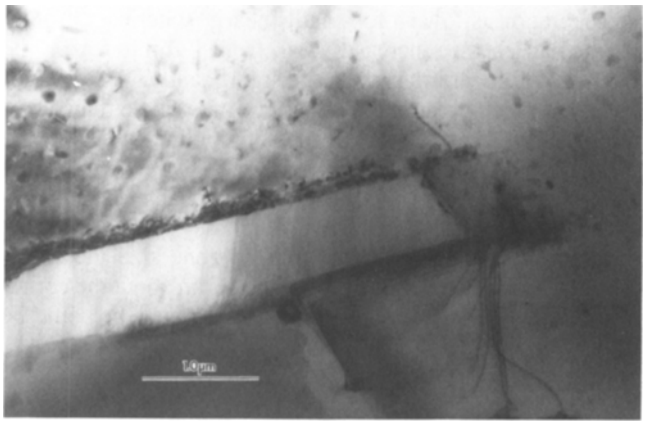

(b)

(c)

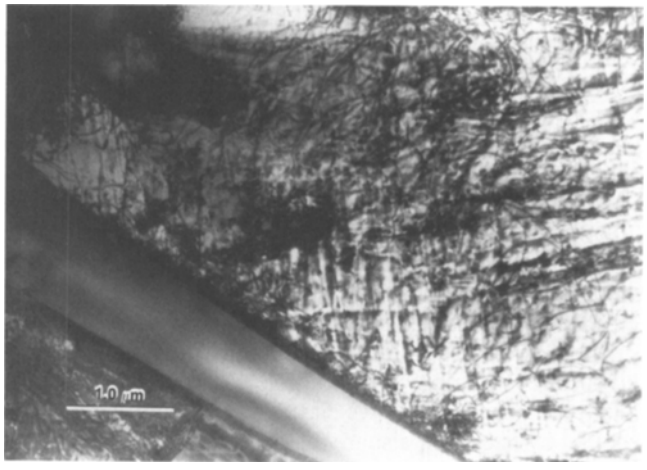

(d)

Fig. 7—(*a*) The diffraction contrast of the high dislocation density in the central subgrain darkens the subgrain in this 20 vol pct SiC platelet composite. The subgrain is surrounded by at least three irregularly shaped SiC platelets which are approximately the same size as the subgrain. (*b*) During heating to 650 K, most of the dislocations disappeared from the sample. The pebble-like second phase precipitates can be clearly distinguished here. The same area is shown in (d) filled with slip traces. (*c*) On cooling to 340 K, dislocations reappeared, resulting in the formation of dense slip traces showing the paths of the dislocations as they moved across or out of the sample. (*d*) This is the same area as shown in (b) after cooling to 340 K. The area was free of almost all dislocations at high temperature. The subgrain is now filled with slip traces and dislocations. The slip traces are clearly associated with the SiC platelets indicating that the origin of the dislocations seen in the sample at low temperature is the Al/SiC interface.

Table I. Dislocation Density before and after Thermal Cycling of Samples; Dislocation Density (m^{-2})

Sample	Before Thermal Cycle	After Thermal Cycle
(1) 20 vol pct whisker†	2.0×10^{13}	1.0×10^{13}
(2) 20 vol pct platelet†	2.0×10^{13}	4.0×10^{12}
(3) 5 vol pct whisker†	4.0×10^{13}	2.0×10^{13}
(4) 0 vol pct whisker†	8.0×10^{12}	6.4×10^{12}
(5) 1100 Al sample*	4.0×10^{12}	5.3×10^{11}

†Bulk annealed 12 hours at 800 K.
*As-received 1100 grade wrought Al alloy.

these mechanisms are operating, which results in a high dislocation density due to the SiC in the matrix. In the vicinity of precipitates, transformation strains can also produce dislocations.

The exception to the generally observed disappearance of dislocations on heating was the 5 vol pct transverse sample for which no satisfactory explanation has been found. A stable polygonized substructure appeared to prevent the disappearance of the dislocations at high temperatures. Backstresses from these dislocations on cooling could have prevented further generation of dislocations in the small subgrains on cooling.

The intensity of dislocation generation at the SiC-Al interface is related to size and shape of SiC particle. The intensity

of generation is lowest for small, nearly spherical particle. As the particle size increases, *i.e.*, from 1 μm to 5 μm, the intensity of generation increases significantly. Also the intensity is much greater at the corner of a particle than along the sides as is evidenced in the longitudinal whisker and platelet composite samples. The relationship between the size of the particle and the plastic zone has been qualitatively described by Lee *et al.*,[15] and they predicted that as the particle size increases the plastic zone size increases. Also, Lee[26] has shown that the plastic strain about the corner of a particle is greater than along the side (which should be intuitively obvious).

Experimental conditions which may influence the results must be recognized and considered in an HVEM experiment, because the sample is exposed to high energy electrons, and thin foil samples are used to approximate bulk behavior. Surface effects are among the most important effects to be considered, since it is easy for dislocations generated at the Al/SiC interface to move out of the sample through the surfaces of a TEM foil. Thick sections of the foil were examined in the HVEM in order to reduce surface effects; nevertheless, dislocation relaxation out the surface occurred, and resulted in a reduction of the observed dislocation density. This effect is most apparent in the 20 vol pct platelet sample where the slip traces, indicating that dislocations have moved out of the sample, nearly cover the entire surface of the sample. In bulk specimens, dislocations would accumulate in the subgrains until the ensuing backstresses due to the pile-up exceeded the local yield stress surrounding the particle. Also, the geometry of a thin foil specimen allows elastic relaxation of stresses on cooling by buckling, also giving an artificially low value of the dislocation density.

The effects of irradiation of the samples by the high energy electrons of the beam must also be considered. Electron irradiation of the sample can result in the formation of vacancy clusters and small dislocation loops which appear as black spots and then grow to form dislocation tangles.[11] The observation of black spots on some of the samples (Figures 1(d) and 6(d)) indicated that electron irradiation damage most probably occurred.

The control samples were invaluable in determining that the dislocations generated on cooling were not artifacts due to the effects of electron irradiation. In the 6061 0 vol pct SiC control sample a few dislocations were generated at a few large precipitates.

The 1100 control samples were also exposed to the high energy electron beam and substantial formation of dislocations did not occur (Figures 3(a) and 3(b)). Also the intensity of dislocation generation can be correlated with the size, volume fraction, and shape of the SiC or second phase precipitate particles present, indicating that the particles and not the electrons of the beam were the cause of the dislocations being generated. A more likely explanation of the appearance of the black spots is beam contamination. The decontaminator was not always operating, and beam contamination usually condenses on samples at temperatures less than 473 K which coincides with our observations.[27,28] Some of the black spots could also be due to second phase precipitation in the samples on cooling, since the spots were sometimes preferentially associated with interfaces and grain boundaries (Figures 1(d) and 7(d)).

Beam heating is another factor to be considered. For our operating conditions, beam heating of the sample is approximately 10 to 15 K, and this could have had an effect on dislocation generation in the sample due to the thermal gradient which is induced.[27,29] But examination of the same composite samples without thermal cycling did not result in dislocation generation at the Al/SiC interface, and these samples were exposed to the same beam conditions.

Due to the difficulty associated with tilting a very fine subgrained material to the various diffracting conditions required to image all of the dislocations in the subgrain, the reported densities could be ⅓ to ½ below the actual number. Although more rigorous tilting would give more precise values, a good idea of the relative densities in the samples can be obtained by imaging dislocations in many subgrains for each material and assuming that the value will be systematically low for all the samples.

The net result of considering all of the experimental factors which may influence the experimentally determined dislocation densities after a thermal cycle, is: (1) the dislocation generation observed during cooling can be readily attributed to differential thermal contraction of the Al and SiC, (2) the observed densities are lower than the densities which would be observed if bulk samples could be examined and if diffracting conditions were controlled to image all dislocations.

It should also be pointed out that slip line generation about a SiC cylinder in an Al disk due to thermal cycling has been demonstrated by Flom and Arsenault.[30]

VI. CONCLUSIONS

From a consideration of the experimental results, the following conclusions can be drawn:

1. The high dislocation density (10^{14} m^{-2}) previously observed in bulk annealed composites is due to differential thermal contraction of Al and SiC on cooling from the elevated temperatures of annealing.
2. The density of dislocations observed in this experiment as a result of thermal cycling is lower than the actual density generated during thermal cycling because dislocations are lost through the surfaces of the thin foil samples during cooling.
3. The densities of dislocations observed (10^{13} m^{-2}) would be equal to the high densities previously observed in bulk annealed composites if it were not for dislocation loss through the surfaces, and the observed densities would be closer to densities predicted by calculations 4×10^{13} m^{-2}, if it were not for dislocation loss through the surfaces.
4. Thermal cycling causes the disappearance of dislocations at high temperatures and the generation of dislocations at Al/SiC interfaces and precipitates on cooling. Subgrain growth is hindered by the presence of SiC particles. Transformation strains also cause dislocation generation at precipitates, and polygonized configurations prevent the disappearance of dislocations at high temperatures.
5. Precipitation occurs on the thermally-generated dislocations during cooling.

ACKOWLEDGMENTS

The authors wish to acknowledge A. Szirmae and J. W. Conroy of the U.S. Steel Research Laboratory, and C. R. Feng and Y. Flom of the University of Maryland for assistance with the experiments. Effective liaison with Drs. Bruce McDonald and Steve Fishman of the Office of Naval Research in Arlington, VA has been very helpful to the project.

REFERENCES

1. M. R. Piggott: *Loading Bearing Fibre Composites*, Pergamon Press, Oxford, 1980.
2. R. J. Arsenault: *Mat. Sci. and Eng.*, 1984, vol. 64, p. 171.
3. R. J. Arsenault and R. M. Fisher: *Scr. Metall.*, 1983, vol. 17, p. 67.
4. A. Taylor and R. M. Jones: *Silicon Carbide*, J. R. O'Connor and J. Smiltens, eds., Pergamon Press, Oxford, 1960, pp. 147-54.
5. K. K. Chawla and M. Metzger: *J. of Mat. Sci.*, 1972, vol. 7, p. 34.
6. K. F. Hale, M. Henderson-Brown, and Y. Ishida: *Proc. 5th European Congress on Electron Microscopy*, 1972, p. 350.
7. D. Caillard and S. L. Martin: *Acta Metall.*, 1983, vol. 31, p. 813.
8. J. K. Kivilahti, V. K. Lindroos, and B. Lehtinen: *Proc. 3rd Int. Conf. on HVEM*, P. R. Swann, C. J. Humphreys, and M. J. Goringe, eds., Academic Press, London, 1974, p. 19.
9. M. Shimotomori and R. R. Hasiguti: *J. Japan Inst. Met.*, 1979, vol. 43, p. 4.
10. A. Wolfenden: *Radiat. Eff.*, 1972, vol. 14, p. 225.
11. J. O. Stiegler and K. Farrell: *Proc. 3rd Int. Conf. on HVEM*, P. R. Swann, C. J. Humphreys, and M. J. Goringe, eds., Academic Press, London, 1974, p. 341.
12. G. C. Weatherly: *Met. Sci. J.*, 1968, vol. 2, p. 237.
13. M. F. Ashby, S. H. Gelles, and L. E. Tanner: *Phil. Mag.*, 1969, vol. 19, p. 757.
14. J. C. Williams and G. Garmong: *Metall. Trans. A*, 1975, vol. 6A, p. 1699.
15. J. K. Lee, Y. Y. Earmme, H. I. Aaronson, and K. C. Russell: *Metall. Trans. A*, 1980, vol. 11A, p. 1837.
16. M. F. Ashby: *Phil. Mag.*, 1970, vol. 21, p. 399.
17. A. Szirmae and R. M. Fisher: "Techniques of Electron Microscopy, Diffraction, and Microprobe Analysis", Special Technical Publ. #372, ASTM, 1965.
18. L. E. Samuels: *Metallographic Polishing Methods*, Sir Issac Pitman & Sons, Ltd., Melbourne, 1971, p. 79.
19. D. G. Howitt: *Analytical Electron Microscopy*, Roy H. Geis, ed., San Francisco Press, San Francisco, CA, 1981, p. 252.
20. P. D. Townsend, J. C. Kelly, N. E. W. Hartley: *Ion Implantation, Sputtering, and Their Applications*, Academic Press, London, 1976, p. 311.
21. G. Dupuoy: "Megavolt Electron Microscopy", *Proc. 3rd Int. Conf. on HVEM*, P. R. Swann, C. J. Humphreys, and M. J. Goringe, eds., Academic Press, London, 1974, p. 447.
22. H. Fujita, T. Tabata, N. Sumida, and K. Yoshida: *Proc. 3rd Int. Conf. on HVEM*, P. R. Swann, C. J. Humphreys, and M. J. Goringe, eds., Academic Press, London, 1974, p. 427.
23. K. F. Hale and M. Henderson-Brown: *Micron*, 1973, vol. 4, p. 69.
24. J. Feng: Master's Thesis, Univ. of Maryland, College Park, MD, 1981.
25. P. B. Hirsch, R. B. Nicholson, A. Howie, D. W. Pashley, and M. J. Whelan: *Electron Microscopy of Thin Crystals*, Butterworth & Co., London, 1965, p. 423.
26. J. Lee: private communications, Michigan Technological University, Houghton, MI, 1984.
27. E. P. Butler and K. F. Hale: "Dynamic Experiments in the Electron Microscope", in *Practical Methods in Electron Microscopy*, Audrey M. Glauert, ed., Elsevier/North Holland Biomedical Press, Amsterdam, 1981, vol. 9.
28. G. M. Scamans and E. P. Butler: *Metall. Trans. A*, 1975, vol. 6A, p. 2055.
29. S. B. Fisher: *Radiat. Eff.*, 1970, vol. 5, p. 239.
30. Y. Flom and R. J. Arsenault: *Mater. Sci. and Eng.*, 1985, vol. 75, p. 151.